Visualization of Poly(ether imide) and Polycarbonate Blending in an Internal Mixer

Bin Lin, Uttandaraman Sundararaj

Department of Chemical and Materials Engineering, University of Alberta, Edmonton T6G 2G6, Canada

Received 3 March 2003; accepted 25 September 2003

ABSTRACT: The blending process of poly(ether imide)/polycarbonate (PEI/PC) was studied by visualization of blending in an internal mixer at 340°C. Distinct pellet deforming, softening, aggregation, stretching, bending, sheeting, and dispersing were seen during the blending process. By ramping the temperature of the barrel of the internal mixer, the process of pellet softening and deforming, and the phase-inversion phenomenon were studied by examining the visualization results and the torque readings. It was found that a peak in torque occurred at the phase-inversion point. It was also found that the blends are semitransparent at higher PEI composition (>80 wt %). SEM and TEM micrographs and DSC data verified the visualization result that PEI/PC blends are partially miscible at higher PEI compositions. The number-average particle size was determined for the PEI/PC blends and it was found that the experimental results in the dilute solution limit for both PC drops and PEI drops did not match with the particle size predicted by Taylor's theory. The particle sizes at 15 wt % concentration were of the same order of magnitude as those calculated using Wu's correlation. © 2004 Wiley Periodicals, Inc. J Appl Polym Sci 92: 1165–1175, 2004

Key words: blends; miscibility; phase inversion; polycarbonates; visualization

INTRODUCTION

Polymer blends provide an effective way to produce new materials—not only are the properties of blends better than those expected from simple mixing rules, but blending is also cheaper than synthesizing a new polymer.[1] High-performance polymer blends are especially attractive because we can combine many desirable properties, and thus these blends are used extensively in industry. It is well known that the blending process is critical in determining the final morphology and final properties of the blend.[2,3] The internal mixer is a very commonly used device in polymer processing. It is used mainly for blending of dissimilar polymers, dispersing fillers, and incorporating dyes or other additives into a polymer matrix or into a polymer blend.[4,5]

Poly(ether imide) (PEI) and polycarbonate (PC) are amorphous high-performance engineering thermoplastics, and their chemical structures are shown in Figure 1. PEI is known to be thermally stable and has extraordinarily good properties, such as excellent high-temperature resistance, toughness, good dielectric properties, low flammability, and high resistance to radiation and deformation under load at elevated temperature. However, it has high melt viscosity,[6,7] and thus can have poor processing characteristics. PC offers toughness and moderate heat resistance, but has a few drawbacks like notch sensitivity.[7,8] The blends of PEI and PC exhibit better mechanical performance than those expected from simple additive rules.[9] Kohlman and Petrie[9] studied the mechanical properties of PEI/PC blends with PEI contents less than 20 wt %. Their study showed that the blends have improved tensile strength, better impact properties, and reduced ductile failure. Chun et al.[10] investigated the thermal properties and morphology of PEI/PC blends. They found that the glass-transition temperature of the PEI-rich phase ($T_{g\,\mathrm{PEI}}$) decreased at the higher PEI weight fractions and a maximum 6°C decrease occurred at 90 wt % PEI, indicating that the blends were partially miscible. Zhang et al.[11] used molecular dynamics to show that PEI/PC blends have anomalous thermodynamic behavior at 80–90 wt % PEI concentration. We will study PEI/PC blends in more detail; specifically, we will visualize the blending process and study the morphology and thermal transitions at different blend ratios.

Visualization is an excellent method to understand polymer pellet deformation, melting, flow, and dispersion. Visualization of drop deformation has been performed successfully on model viscoelastic fluids and polymers in different flow fields. Examples of work on model fluids include the following: Han and Funatsu[12] studied glycerin drop deformation in a pressure-driven shear flow; Peuvrel and Navard[13] ob-

Correspondence to: U. Sundararaj (u.sundararaj@ualberta.ca).
Contract grant sponsor: Natural Sciences and Engineering Research Council of Canada.

Journal of Applied Polymer Science, Vol. 92, 1165–1175 (2004)

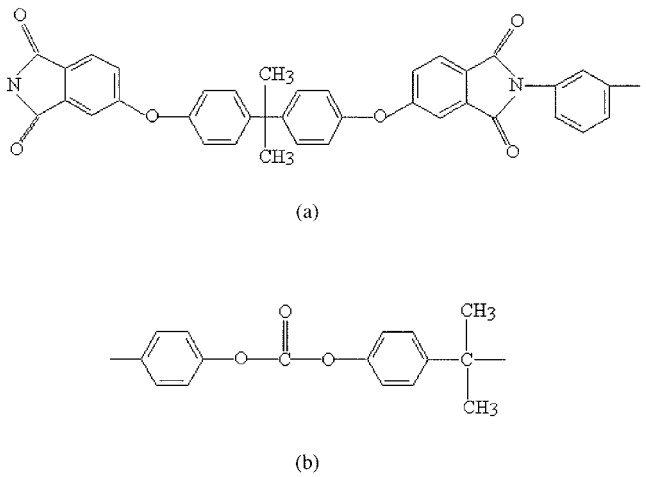

Figure 1 Chemical structure of (a) PEI and (b) PC.

tained the velocity profile of a hydroxypropylcellulose drop in a cone-and-plate device; Shih et al.[14] observed glass fiber dispersion in corn syrup solution in a twin-screw extruder (TSE); Mighri et al.[15]used transparent parallel plates to observe the deformation and critical breakup of Boger fluid drops; Jaffer et al.[16] viewed the velocity field in a transparent TSE using mineral oil; and Mighri and Huneault[17] studied the drop deformation and breakup using model fluids in a transparent Couette cell.

Examples of polymer flow visualization include the following: Sundararaj et al.[18] and Levitt et al.[19] investigated the initial breakup mechanisms of polymer blends by observing polymer pellet deformation between two parallel plates; Archer et al.[20] visualized the slip flow of silica spheres in PS (polystyrene) solutions using a glass Couette device; Sakai[21] observed HDPE (high-density polyethylene) melting through a glass window on an extruder; Gogos et al.[22] studied PS/LDPE (low-density polyethylene) and LDPE/PS blends in a model mixer (twin-screw mixing element evaluator); Migler et al.[23] viewed PS drop deformation in PE (polyethylene) in channel flow at the die of the extruder; and Lin et al.[24,25] studied polymer drop breakup mechanisms in a heated counterrotating Couette device.

Important aspects of the mixing process have been established by visualizing through a transparent glass window in the front of an internal mixer.[26–32] Min and White[26] studied the flow behavior of elastomers and molten plastics in a Banbury-type mixer. They observed the stretching, tearing, "sheeting out," and banding in elastomers, and "sheeting out" in plastics. The "sheeting out" phenomenon was observed as the colored sample sheet is sheared as a thin film layer on the chamber wall. Shih et al.[27] investigated the melting and softening behavior of nylon, polyethylene, and polystyrene in an internal mixer with roller blades. They identified four distinct rheological characteristics during the blending process:

1. Elastic solid pellets
2. Deformable solid pellets
3. Transitional material, such as powdery or doughlike material
4. Viscoelastic fluid

Later, Shih[28] studied the phase-inversion phenomenon in polymer blends composed of a plastic material with a high softening temperature as the major phase (>60 wt %) and a rubbery material with a low softening temperature as the minor phase (<40 wt %). The rubber initially formed the continuous phase and the major phase polymer with the higher softening temperature broke up inside the rubbery phase. It was found that in the region of maximum torque, an abrupt phase inversion occurs; consequently, finely dispersed rubber droplets were enclosed by the major phase polymer. The observation[28] of the phase inversion at the maximum torque has been seen in many polymer blends.[28–31,33–35] Generally, the phase inversion occurs when the minor phase has a lower softening or melting temperature,[28–30,33,35] or a low viscosity ratio (<0.2).[31,34,35]

There are two equations frequently used by polymer blending researchers to estimate the final dispersed particle size of the blends: (1) the Taylor limit[36] and (2) Wu's correlation.[37] Taylor[36] studied a single Newtonian drop in another Newtonian liquid subjected to simple shear flow. By balancing the interfacial force and the shear force, he predicted the maximum drop size that would be stable for small deformations in Newtonian fluids:

$$D = \frac{4\Gamma(\eta_r + 1)}{\dot{\gamma}\eta_m\left(\frac{19}{4}\eta_r + 4\right)} \qquad \eta_r < 2.5 \tag{1}$$

where D is the drop diameter, $\dot{\gamma}$ is the shear rate, Γ is the interfacial tension, η_m is the viscosity of the matrix or major phase, η_d is the viscosity of the drop or the minor phase, and $\eta_r = \eta_d/\eta_m$ is the viscosity ratio. This relation is valid for all small deformations in Newtonian fluids when $\eta_r < 2.5$. Taylor predicted[36] that no drop breakup will occur when $\eta_r > 2.5$. The dimensionless number that characterizes drop breakup is the capillary number:

$$\mathrm{Ca} = \frac{\dot{\gamma}\eta_m D}{2\Gamma} \tag{2}$$

The capillary number is a ratio of the shear stress to the interfacial stress and can be thought of as an effective shear rate experienced by the drop.

TABLE I
Properties of Polymers Used

Polymer (abbreviation)	Molecular weight (M_w)[a]	Density, ρ (kg/m^3)		Viscosity at 340°C[c] γ = 65 s^{-1} (Pa s)	Glass-transition temperature, T_g (°C)[d]
		25°C[a]	340°C[b]		
Poly(ether imide) Ultem 1000	30,000	1270	1140	2850	217
Polycarbonate Lexan 141	28,450	1200	1020	210	150

[a] Provided by supplier.
[b] Calculated from group contribution, from Ref. 38.
[c] Measured in RMS 800 with a 25-mm parallel-plate fixture at 10% strain.
[d] Measured with TA Instruments DSC 2910.

Wu's correlation[37] is based on the final particle diameter of extruded polymer blends with minor phase concentration of 15 wt %:

$$D = \frac{4\Gamma\eta_r^{\pm 0.84}}{\dot{\gamma}\eta_m} \quad (3)$$

where the plus (+) sign in the exponent applies for $\eta_r > 1$ and the minus (−) sign applies for $\eta_r < 1$. It is important to note that this is a correlation and has no theoretical basis.

In this study, we visualized the blending process of PEI/PC in an internal mixer with roller blades using a quartz window in front of an internal mixer. We characterized distinct deformation and softening periods and several transitions in blend consistency as the melt blend reached the final homogeneous state.

EXPERIMENTAL

Materials

Two kinds of polymers, poly(ether imide) (PEI, Ultem 1000) and polycarbonate (PC, Lexan 141), were used in the experiments. Both were kindly provided by GE Plastics (Pittsfield, MA). Table I gives some of the physical properties of the polymers. The properties were either measured or calculated from group contribution methods.[38] All the polymer pellets used in the experiments were dried in a vacuum oven overnight at 90°C.

Blending

The internal mixer was a Haake Rheomix series 600 batch mixer (Haake, Bersdorff, Germany), shown schematically in Figure 2. The mixer was connected to a Rheocord90 control panel. A quartz window was designed for the front plate of the mixer through which the blending process was easily observed and recorded using a video camera. Before blending, the mixer was preheated to the required barrel temperature and the rotors were set to the desired rotation rate. Most experiments were run at 50 rpm and 340°C. A value of 50 rpm corresponded to a maximum shear rate of 65 s^{-1} in the minimum gap of the mixer. In this blend system, PEI had a viscosity of 2850 Pa s^{-1} and PC had a viscosity of 210 Pa s^{-1} at a shear rate of 65 s^{-1} at 340°C.

PEI and PC are amorphous; therefore, each polymer by itself is transparent. PEI has a high glass-transition temperature (T_g = 217°C) and PC has a lower glass-transition temperature (T_g = 150°C) (see Table I for a summary of properties). The PEI/PC blends were prepared using the following procedure unless otherwise specified. To reduce degradation, 0.1 wt % Irgafos 168 stabilizer [tris(2,4-di-*tert*-butylphenyl)-phosphite (Ciba Specialty Chemicals, Summit, NJ)] was added to the blends. To avoid the phase-inversion phenomenon during blending,[29] when PEI was the major component (>60 wt %), PEI pellets were added through the feed chute into the mixer chamber first and PC pellets

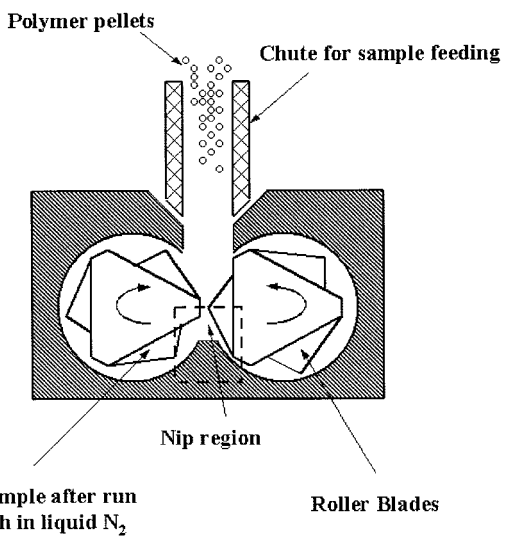

Figure 2 Batch mixer cross section. A specially designed quartz window was used in front of the mixer for visualization. The mixing was viewed best in the nip region.

were added 2 min later, when PEI pellets were already softened. The PEI was premixed with stabilizer before it was added into the mixer. This blending procedure simulated downstream feeding of PC in an extruder. However, when PEI was the minor phase (<40 wt %), PEI pellets and PC pellets were premixed with the stabilizer and then added together into the empty mixer chamber. The total melt volume was 75% of the mixer volume. At the end of the run, the mixer was disassembled, and the blend sample was extracted quickly from the indents in the blades and quenched in liquid nitrogen.

Scanning electron microscopy and image analysis

The morphology of the fractured surface of the blend sample was analyzed using a Hitachi S2700 scanning electron microscope (SEM; Hitachi, Osaka, Japan) with Princeton Gamma Tech (PGT) Imix imaging software. The fractured surfaces of the samples were initially sputter coated with gold before imaging in the SEM. The micrographs were taken at an accelerating voltage of 20 kV.

The particle size of the dispersed phase was measured with SigmaScan Pro (version 4.01) software. The area (A) of each particle was determined and the equivalent diameter was obtained by assuming that the particle cross section was circular in shape, that is,

$$D_{eq} = \sqrt{\frac{4A}{\pi}} \tag{4}$$

This equivalent diameter (D_{eq}) was used to obtain the number-average diameter (D_n):

$$D_n = \frac{\sum_{i=1}^{n} D_{eq,i}}{n} \tag{5}$$

where n is the number of particles. Several SEM micrographs were used to determine the average diameter of each sample. For low concentrations (<5%), about 50–100 particles were averaged, and for high concentrations, about 150–200 particles were used. The calculated diameters were used to evaluate the effect of composition on particle size.

Transmission electron microscopy

The morphology of the cross section of the blends was analyzed using a Philips CM12 transmission electron microscope (TEM; Philips. The Netherlands) at an operating voltage of 80 kV. The samples were stained with ruthenium tetroxide (RuO_4) before imaging with the TEM.

Differential scanning calorimetry measurements

Differential scanning calorimetry (DSC) experiments were carried out in a TA Instruments DSC 2910 calorimeter (TA Instruments, New Castle, DE). The blend samples (5–10 mg) were heated under nitrogen at a scanning rate of 10°C/min from 100 to 280°C. The glass-transition temperatures of the PEI-rich phase ($T_{g\,\mathrm{PEI}}$) and the PC-rich phase ($T_{g\,\mathrm{PC}}$) were obtained from the first heating scan.

RESULTS AND DISCUSSION

Visualization and torque analysis

Figure 3 shows the blending process of PEI/PC (85 : 15 wt %) in the nip region of the batch mixer (mixer nip region schematically shown in Fig. 2). Zero time corresponds to the time when PEI pellets are first fed into the mixer. Separate, distinct PEI pellets are seen at the beginning of the mixing [Fig. 3(a)]. The pellets soften and aggregate at approximately 20 s because of the heating and shearing in the batch mixer [Fig. 3(b)]. The aggregates continue to grow into more cohesive lumps [Fig. 3(c)], and transform into viscous "taffy candy"–like material that is stretched out by the rotor motion [Fig. 3(d), (e)]. The viscous "taffy" incorporates and forms a viscoelastic fluid-like material. The PC pellets are added into the mixer at 2 min [Fig. 3(f)], and the PC pellets are softened and deformed almost immediately [Fig. 3(g)]; no distinct PC pellets are seen even after only 10 s of further mixing [Fig. 3(h)]. Again, this blend protocol parallels an extrusion process when PEI is fed at the throat of the extruder and PC is fed downstream at a location where the PEI has already softened. As indicated in our earlier study,[32] the final blend is not opaque, but rather is a hazy mixture. Visualization of several other compositions of PEI/PC blends (80 : 20, 90 : 10, 95 : 5, 96 : 4, 98 : 2, and 99 : 1) also showed semitransparent blends, which indicates that the blends may be partially miscible at high PEI compositions. As the PEI composition increases, the transparency of the final blend also increases. The particle size and concentration of the dispersed phase may also influence the transparency of the blend. PEI/PC blends at high PC concentrations (PEI/PC concentration 1 : 99; 5 : 95; 10 : 90; 20 : 80) were made for SEM, TEM, and DSC analysis.

Figure 4 presents visualization micrographs showing the deformation and transition phenomena during the blending process of PEI/PC (80 : 20) at a slower rotation speed of 10 rpm. At a time of about 40 s, the PEI pellets aggregate together—some of them are completely softened and some seem to have solid cores at the center of the pellets [Fig. 4(a)]. The pellets continue to deform, the pellets are stretched out, and the "sheeting out" phenomenon[18,24,39] occurs [Fig. 4(b)]. The stretching occurs even after the PEI is soft-

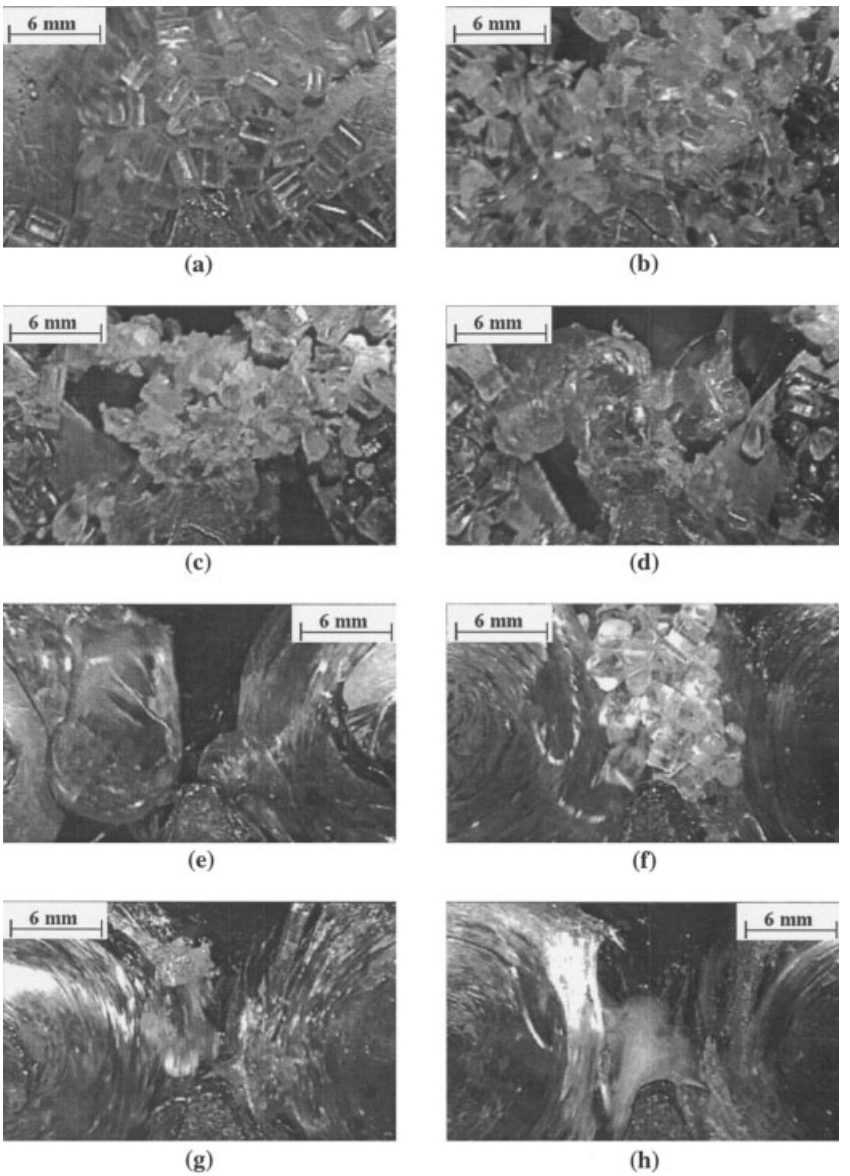

Figure 3 PEI/PC (85 : 15 wt %) blending at 340°C, 50 rpm. PEI added first. Note the scale bar. (a) Distinct PEI pellets (t = 4 s); (b) agglomerated PEI pellets (t = 26 s); (c) cohesive PEI lumps (t = 29 s); (d) taffy candy melt (t = 32 s); (e) viscoelastic PEI melt (t = 42 s); (f) distinct PC pellets (t = 123 s); (g) softened and deformed PC pellets (t = 127 s); (h) PC dispersed into PEI melt (t = 133 s).

ened [Fig. 4(c)]. After the PC pellets are added into the softened PEI phase, the PC pellets are stretched and deformed very quickly even at this low rotation speed [see Fig. 4(d)].

By slowly increasing the barrel temperature of the mixer during mixing, we can more clearly distinguish the deformation and melting processes. Runs with temperature ramping more closely follow the temperature profile in an extruder (i.e., the mixing time in the internal mixer parallels the length down the extruder). Figure 5 plots barrel temperature, melt temperature, and torque versus time for a temperature ramp run for PEI/PC (85 : 15) mixed at 50 rpm. Figure 6 shows the corresponding images taken at the points indicated in Figure 5. At the beginning of the experiments, the barrel temperature is set at 100°C for 3 min, and then it is increased by 5°C/min to 360°C. In this run, PEI pellets, PC pellets and Irgafos 168 stabilizer are premixed at room temperature and then fed into the mixing chamber. Because PC (15%) softens before the PEI (85%), a phase inversion should occur in this system during the blending.

A sharp first peak (Fig. 5) in torque occurs just after feeding, which is attributed to the stiffness of PEI pellets at this low temperature (100°C). This peak decreases as the barrel temperature is continuously increased. A second small peak [point (a)] occurs at a melt temperature of 155°C and the corresponding pic-

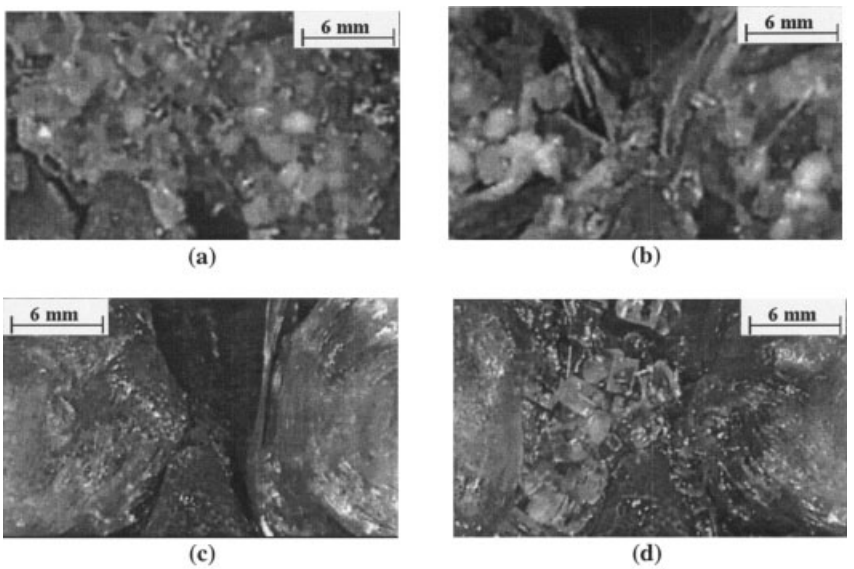

Figure 4 PEI/PC (80 : 20 wt %) blending at 340°C, 10 rpm. PEI added first. Note the scale bar. (a) Agglomerated PEI pellets (t = 38 s); (b) stretching and sheeting out of the deformed PEI pellets (t = 48 s); (c) stretching of PEI melt (t = 117 s); (d) deformation and stretching of PC pellets (t = 148 s).

ture is shown in Figure 6(a). At this point, PEI pellets are still rigid, whereas the PC pellets are starting to deform (indicated with white circles in the figure) because PC has a lower T_g than that of PEI (see Table I). The second torque peak suggests that some energy input is required to deform and soften PC pellets. The mechanical energy from the mixer motor is converted to thermal energy that softens the PC pellets. The softened PC phase coats the PEI pellets. After PC completely softens, a third peak [point (b)] appears at a melt temperature of 223°C, about 6°C higher than the glass-transition temperature of PEI. As shown in Figure 6(b), PEI pellets begin to soften and deform at this point. PEI pellets continue to soften and aggregate as the temperature is increased [Fig. 6(c)]. The pellets in the aggregates are bent and stretched [point (d) in Fig. 5 and the micrograph in Fig. 6(d)]. After another 6°C increase in the melt temperature, the PEI pellets merge together [point (e) on the torque trace] and the torque reaches a local minimum. After point (e), a sharp increase in torque occurs. During this stage, PEI and PC are merging and the mixture has a "mashed potato"–like consistency and appearance [Fig. 6(f), (g)]. In the "mashed potato" stage, the polymer blend seems dry and powdery [Fig. 6(f)], suggesting imperfect mixing. The mixture looks more cohesive and homogeneous at a melt temperature of 260°C [Fig. 6(g)], where a maximum torque of 34.6 N m^{-1} is achieved. The fourth peak in the torque occurs at the point of the beginning of phase inversion in the blend.[28–31,33–35] The blends transform into a viscoelastic melt soon after experiencing this high torque [Fig. 6(h)].

SEM analysis

Figure 7 shows the SEM micrographs of PEI/PC blends and Figure 8 gives the dispersed phase particle size and standard deviation calculated from SEM micrographs. If PC is the major phase [e.g., Fig. 7(a) and (b)], the dispersed-phase particles have a larger size [$D_n > 1$ μm; see Fig. 8(a)] than that if PEI is the major phase [$D_n < 1$ μm; see Fig. 8(a) and (b) and micrographs in Fig. 7(c)–(f)]. This is partly because the viscosity of PEI is much higher than that of PC (Table I); thus the viscosity ratio is 13.6 when PC is the major phase and 0.07 when PEI is the major phase. It was

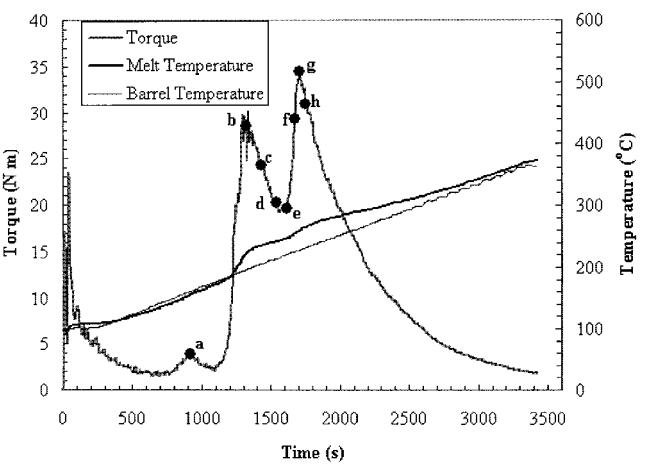

Figure 5 Temperature and torque profiles for PEI/PC (85 : 15 wt %) blending at 50 rpm, temperature ramp from 100 to 360°C. The points (a)–(h) on the torque curve correspond to micrographs in Figure 6(a)–(h).

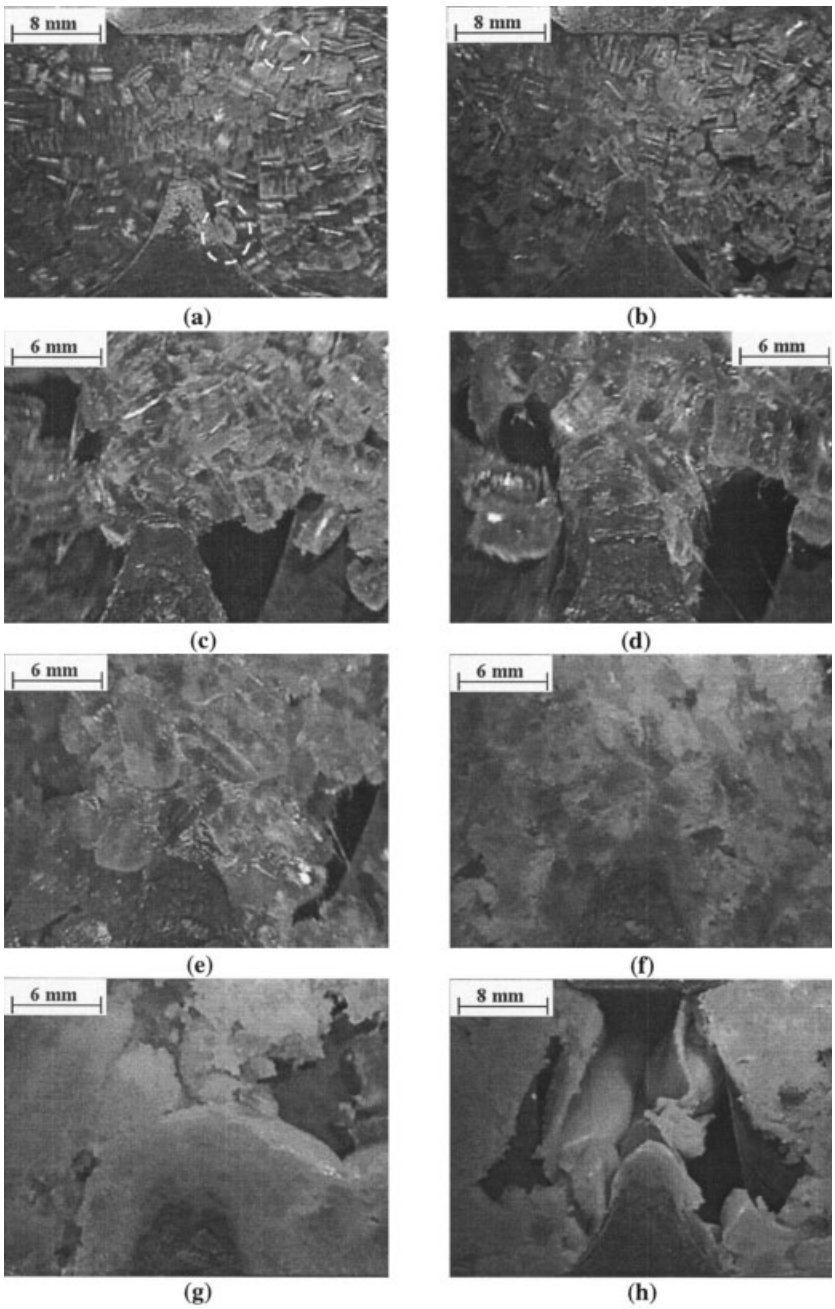

Figure 6 PEI/PC (85 : 15 wt %) blending at 50 rpm with temperature ramp shown in Figure 5. All materials added together. Note the scale bar. (a) Solid PEI pellets and deformed PC pellets—the dotted white circles indicate some of the deformed PC pellets (t = 918 s, T_m = 155°C, T = 3.9 N m^{-1}); (b) softened PC coats PEI pellets and PEI pellets begin to deform (t = 1320 s, T_m = 223°C, T = 28.6 N m^{-1}); (c) solid PEI/PC aggregate (t = 1431 s, T_m = 235°C, T = 24.3 N m^{-1}); (d) viscous PEI/PC aggregate (t = 1545 s, T_m = 242°C, T = 20.3 N m^{-1}); (e) softened lumps (t = 1624 s, T_m = 248°C, T = 20.1 N m^{-1}); (f) "mashing potato" (t = 1674 s, T_m = 254°C, T = 29.3 N m^{-1}); (g) "mashed potato," torque is highest at this point (t = 1706 s, T_m = 260°C, T = 34.6 N m^{-1}); (h) viscoelastic melt (t = 1756 s, T_m = 266°C, T = 31.2 N m^{-1}).

previously shown by Favis and Chalifoux[40] that a larger dispersed drop size is expected at higher viscosity ratio.

At 20% PC, the particle size (D_n) is about 0.7 μm; however, when the PC content is decreased to 10%, the PC D_n decreases to about 0.3 μm. The large difference in particle size is most probably attributable to the increased coalescence of PC drops at higher PC concentrations. The small particle size at high PEI contents ($D_n < 1$ μm) may also suggest why the blends are semitransparent at these blend ratios.

The SEM micrographs show that, at a concentration of 99% PEI, no particles can be seen [Fig. 7(f)]. This explains why the blend is almost transparent at high

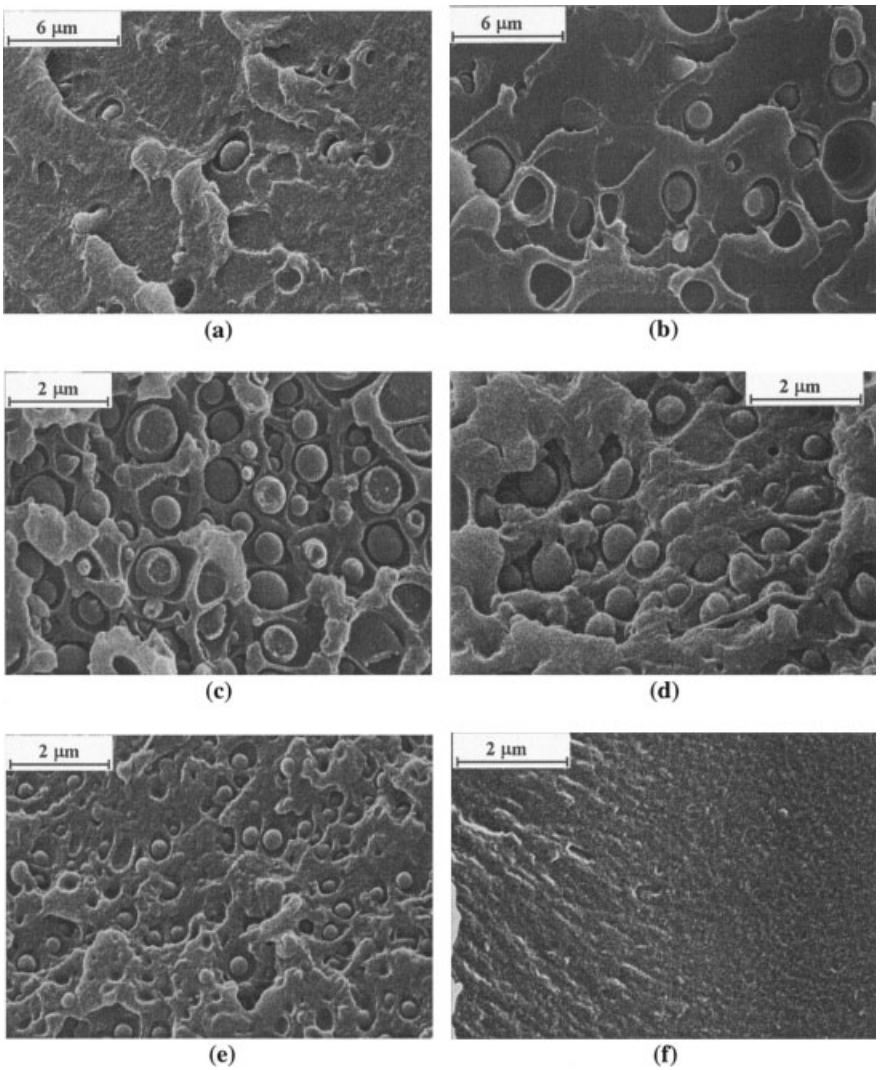

Figure 7 Scanning electron micrographs of PEI/PC blends with a PEI : PC composition of (a) 1 : 99, (b) 20 : 80, (c) 80 : 20, (d) 85 : 15, (e) 90 : 10, and (f) 99 : 1. No particles could be discerned for the PEI/PC 99 : 1 blend. Note that the magnifications for (a) and (b) are lower than those for the other micrographs. See scale bars in each micrograph.

PEI contents; all the PC has been completely incorporated into PEI. However, when the blend has 99% PC [Fig. 7(a)], PEI particles are still visible ($\sim$ 1 μm), suggesting that two distinct phases exist at high PC contents.

TEM analysis

Two TEM micrographs of blends, one with high PEI content and one with high PC content, are presented in Figure 9. In Figure 9(a), the blend has PC in majority with a composition of 85% and in Figure 9(b), the blend has PEI in majority with a composition of 85%. The RuO_4 stains and darkens the PC phase, but does not stain the PEI phase very much. So, in a typical micrograph, the black phase is PC and the white phase is PEI.

Figure 9(a) shows white PEI particles dispersed in a black PC matrix phase. However, Figure 9(b) reveals that there is no pure white PEI phase, but rather there is a "gray phase," or a combination of white and black. Therefore, some PC has already been incorporated into the PEI phase, creating a mixed phase that is stained gray. That is, the two polymers are partially miscible when PEI is the major phase. Pure PEI samples stained with RuO_4 for the same time show a pure white phase. At low PC contents (1 wt %), a gray phase is seen with no discernable PC particles, indicating that all the PC has been incorporated into PEI.

The TEM micrographs also verify the SEM results that the dispersed particle size is larger when PEI is the minor phase [Fig. 9(a), $D_n > 1$ μm] and smaller when PEI is the major phase [Fig. 9(b), $D_n < 1$ μm], which is attributed to the different viscosity ratio for

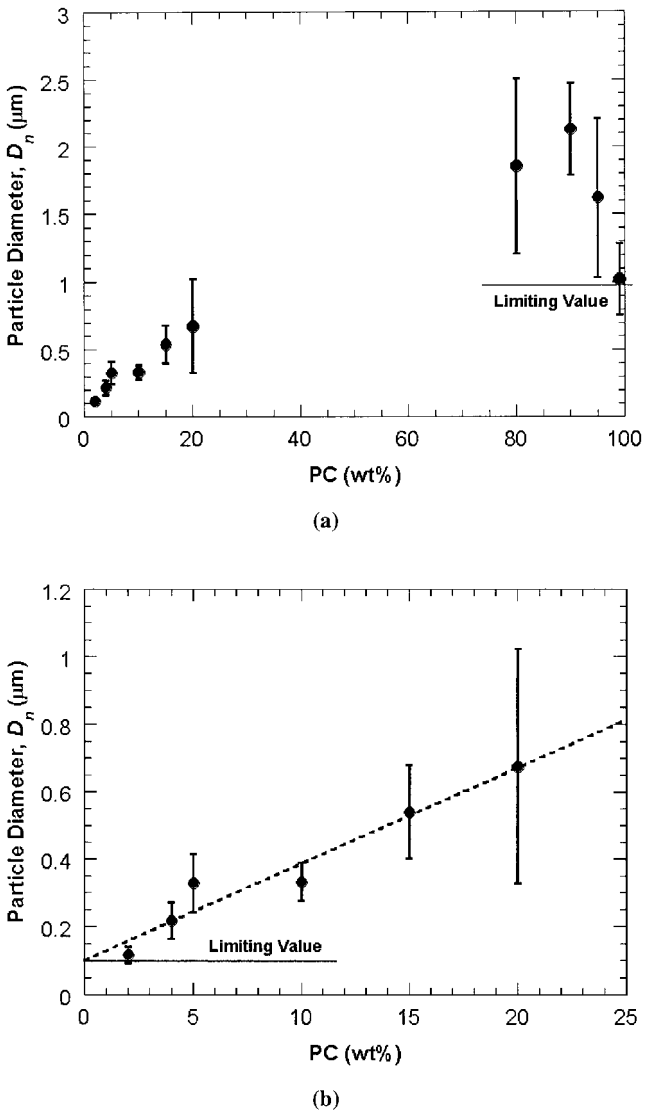

Figure 8 (a) Particle size of dispersed phase in PEI/PC blends obtained from SEM at different compositions; (b) enlarged plot at low PC concentration. The "error bars" are 1 SD of the particle size distribution in each direction.

the two cases.[40] Table II shows the results of the limiting particle size compared to the Taylor[36] limit [eq. (1)] and the particle size at 15 wt % compared to the Wu[37] correlation [eq. (3)]. The interfacial tension (Γ) between PC and PEI is calculated as $\Gamma = 0.76$ mN/m at 340°C using the harmonic-mean equation suggested by Wu.[41] The equation relates the interfacial tension to the surface tension and the polarity of the two contiguous phases. The Taylor[36] limiting particle size corresponding to the dilute solution limit is very small (0.004 μm) for PC drops in PEI but does not match well with the limiting value obtained from experiments (0.10 μm). For micrographs of 1% PC in PEI, we were unable to see particles because the two materials were miscible. For PEI drops, eq. (1) predicts no breakup but experiments give a limiting particle size of 1.0 μm. It is clear from these results that the Taylor limit cannot be applied for polymer systems.[42] However, the experimentally determined diameters at 15 wt % of the minor phase are of the same order of magnitude as diameters calculated from Wu's correlation.[37] This is because the blends from the internal mixer should have a morphology similar to that obtained from extruders.[3,43]

DSC analysis

Figure 10(a) shows the DSC measurements of T_g for the PEI-rich phase. The T_g has a minimum at PC content of approximately 15%. The largest difference in glass-transition temperature is about 6°C, which is similar to the findings of Chun et al.[10] However, in our study, the glass-transition temperature in the high PEI content blends decreases with increasing PC compositions up to 15% (not 10% as reported by Chun et al.[10]), and then increases back to the pure PEI glass-transition temperature upon further increase in PC content. Little change in $T_{g\,\mathrm{PEI}}$ is observed at PC composition greater than 40%. Figure 10(b) shows the glass-transition temperatures of both the PEI-rich phase and PC-rich phase as a function of the weight fraction of PC. Very little change is observed in $T_{g\,\mathrm{PC}}$ for the range of blend concentration studied.

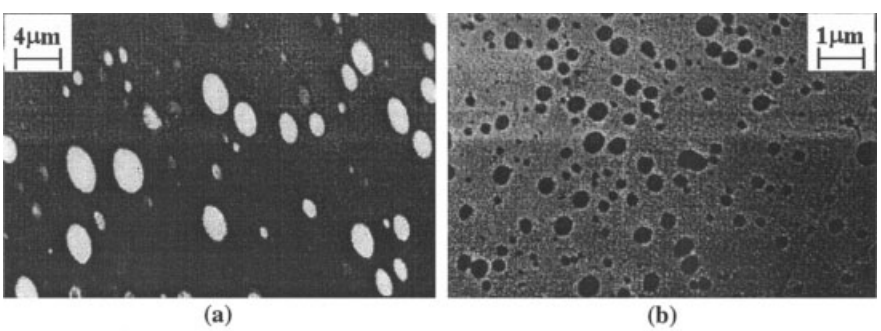

Figure 9 Transmission electron micrographs of PEI/PC blends with a PEI : PC composition of (a) 15 : 85 and (b) 85 : 15. Note that the magnification for micrograph (a) is lower than that for micrograph (b). See scale bars in each micrograph.

TABLE II
Comparison of Dispersed Particle Size

Major phase	D_n limiting value (μm)	Taylor limit[a] (μm) [eq. (1)]	D_n at 15% minor phase (μm)	Wu correlation[b] (μm) [eq. (3)]
PEI	0.10	0.004	0.54	0.15
PC	1.0	Not applicable (predicts no breakup)	2.0	2.0

[a] Ref. 36.
[b] Ref. 37.

The shift in $T_{g\,\mathrm{PEI}}$ to a lower temperature at higher PEI compositions indicates partial miscibility of PEI/PC blends at these blend ratios.[11,44] According to Kim and Burns,[45] by reformulating the Fox equation, it is possible to calculate the apparent weight fractions of polymer components in each phase of the partially miscible blends:

$$\frac{1}{T_g'} = \frac{w_1'}{T_{g1}} + \frac{w_2'}{T_{g2}} \tag{6}$$

$$\frac{1}{T_g''} = \frac{w_1''}{T_{g1}} + \frac{w_2''}{T_{g2}} \tag{7}$$

$$w_1' + w_2' = 1 \tag{8}$$

$$w_1'' + w_2'' = 1 \tag{9}$$

When we apply these equations to the PEI/PC blends, subscript 1 represents PEI and subscript 2 represents PC; the superscripts $'$ and $''$ represent the PEI-rich phase and the PC-rich phase, respectively; T_g' is the glass-transition temperature of the PEI-rich phase; T_g'' is the glass-transition temperature of the PC-rich phase; T_{g1} and T_{g2} are the glass-transition temperatures of the pure PEI and pure PC, respectively; and w is the apparent weight fraction.

Table III shows the calculation results for the apparent weight fraction of PC in the PEI-rich phase (w_2') and PEI in the PC-rich phase (w_1'') using eqs. (6)–(9). It was found that the apparent weight fraction of PC in the PEI-rich phase changes from 6 to 2% as the weight fraction of PC in the blend is increased from 15 to 30%. When the PC weight fraction exceeds 40% in the blend, there is negligible PC (<1%) in the PEI-rich phase. It was also found that the apparent weight fraction of PEI in the PC-rich phase is almost zero for all the blends studied. Therefore, PC is incorporated into the PEI-rich phase at high PEI compositions

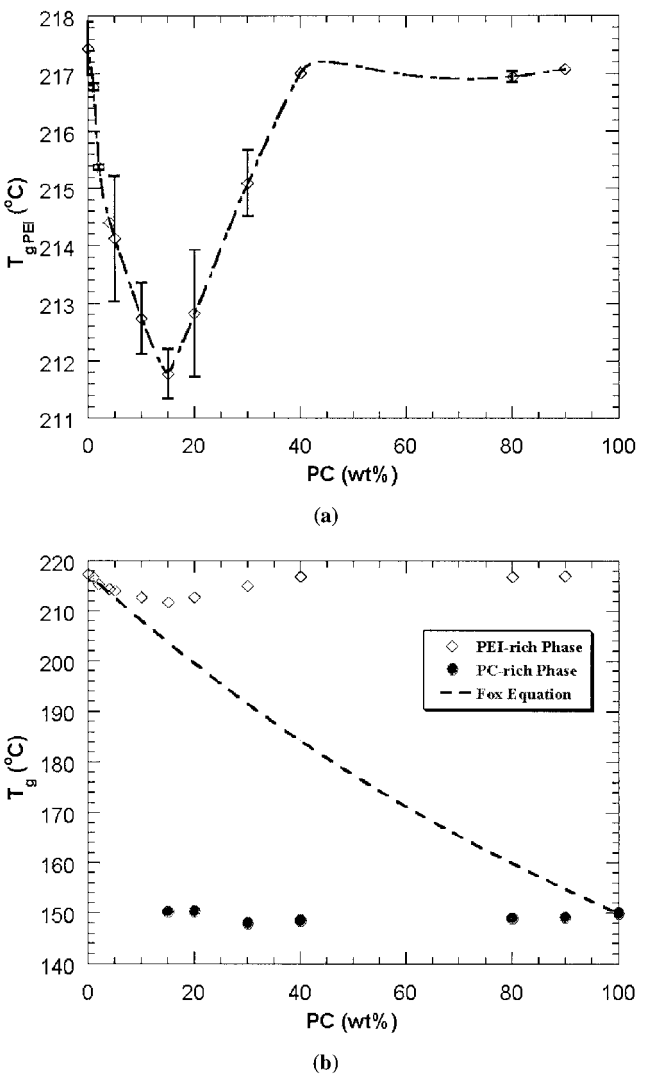

Figure 10 Glass-transition temperature of: (a) PEI-rich phase only and (b) PEI-rich and PC-rich phases as a function of PC weight fraction for PEI/PC blends. Curve in (b) was obtained using Fox equation.

TABLE III
Apparent Weight Fractions of PC in PEI-Rich Phase (w_2') and PEI in PC-Rich Phase (w_1'')

	PC (wt %)					
Phase	15	20	30	40	80	90
w_2'	0.06	0.05	0.02	0.00	0.00	0.00
w_1''	0.01	0.01	0.00	0.00	0.00	0.00

(≥70%); however, there is no PEI incorporated into the PC-rich phase. This may be attributable to the fact that the PEI-rich phase will freeze at a higher temperature, perhaps trapping some of the PC.[46] However, the PC phase can separate further because it does not freeze until a much lower temperature. Therefore, it is possible for one phase to be diluted by the other polymer, and this separation phenomenon[46] may describe the $T_{g\,\mathrm{PEI}}$ decrease seen in our experiments.

CONCLUSIONS

The high-temperature (340°C) blending process of PEI/PC blends in an internal mixer was visualized through a quartz window in the front of the mixer. The solid pellets underwent distinct softening, deforming, bending, aggregating, sheeting, and stretching before a viscoelastic melt consistency was achieved. The same transitions are expected to occur in an extrusion process. PEI/PC blends also showed several distinct deformation and softening regimes and exhibited phase inversion at high PEI content when the PEI and PC were added together. Unique blend textures like "taffy candy melt" and "mashed potato" were observed and corresponded to transitions/peaks in the torque rheology. The final blends at high PEI compositions were semitransparent, suggesting the PEI/PC blends are partially miscible at high PEI concentrations. Partial miscibility at high PEI concentrations was verified by SEM and TEM micrographs, where PC was seen to incorporate into the PEI-rich phase, and by DSC analysis, which showed a decrease in the T_g of the PEI-rich phase at high PEI levels.

The authors thank the Natural Sciences and Engineering Research Council of Canada for supporting this research, and also thank Tina Barker for performing SEM analysis and Mingzong Zhang for preparing some of the blends.

References

1. Utracki, L. A. Polymer Alloys and Blends; Hanser Publishers: Munich, 1989.
2. Utracki, L. A.; Shi, Z. H. Polym Eng Sci 1992, 32, 1824.
3. Sundararaj, U.; Macosko, C. W.; Rolando, R.; Chan, H. T. Polym Eng Sci 1992, 32, 1814.
4. Middleman, S. Fundamentals of Polymer Processing; McGraw-Hill: New York, 1977.
5. Tadmor, Z.; Gogos, C. G. Principles of Polymer Processing; Wiley: New York, 1979.
6. Serfaty, I. W. In: Polyimides; Mittal, K. L., Ed.; Plenum Press: New York, 1984; Vol. 1, p 149.
7. Fried, J. R. Polymer Science and Technology; Prentice Hall: Englewood Cliffs, NJ, 1995.
8. Kulshreshtha, A. K. Polym Plast Technol Eng 1993, 32, 551.
9. Kohlman, W. C.; Petrie, S. P. Adv Polym Technol 1995, 14, 111.
10. Chun, Y. S.; Lee, H. S.; Kim, W. N.; Oh, T. S. Polym Eng Sci 1996, 36, 2694.
11. Zhang, M.; Choi, P.; Sundararaj, U. Polymer 2003, 44, 1979.
12. Han, C. D.; Funatsu, K. J Rheol 1978, 22, 113.
13. Peuvrel, E.; Navard, P. Macromolecules 1990, 23, 4874.
14. Shih, C.-K.; Royer, D. J.; Tynan, D. G. SPE ANTEC Tech Papers 1995, 53, 2413.
15. Mighri, F.; Carreau, P. J.; Ajji, A. J Rheol 1998, 42, 1477.
16. Jaffer, S. A.; Bravo, V. L.; Wood, P. E.; Hrymak, A. N.; Wright, J. D. Polym Eng Sci 2000, 40, 892.
17. Mighri, F.; Huneault, M. A. J Rheol 2001, 45, 783.
18. Sundararaj, U.; Dori, Y.; Macosko, C. W. SPE ANTEC Tech Papers 1994, 52, 2448.
19. Levitt, L.; Macosko, C. W.; Pearson, S. D. Polym Eng Sci 1996, 36, 1647.
20. Archer, L. A.; Larson, R. G.; Chen, Y. L. J Fluid Mech 1995, 301, 133.
21. Sakai, T. Adv Polym Technol 1995, 14, 227.
22. Gogos, C. G.; Essenghir, M.; Todd, D. B.; Yu, D. W. Macromol Symp 1996, 101, 185.
23. Migler, K. B.; Hobbie, E. K.; Qiao, F. Polym Eng Sci 1999, 39, 2282.
24. Lin, B.; Sundararaj, U.; Mighri, F.; Huneault, M. A. Polym Eng Sci 2003, 43, 891.
25. Lin, B.; Mighri, F.; Huneault, M. A.; Sundararaj, U. Macromol Rapid Commun 2003, 24, 783.
26. Min, K.; White, J. L. Rubber Chem Technol 1985, 58, 1024.
27. Shih, C.-K.; Tynan, D. G.; Denelsbeck, D. A. Polym Eng Sci 1991, 31, 1670.
28. Shih, C.-K. Polym Eng Sci 1995, 35, 1688.
29. Sundararaj, U.; Macosko, C. W.; Shih, C. K. Polym Eng Sci 1996, 36, 1769.
30. Sundararaj, U. Macromol Symp 1996, 112, 85.
31. Ratnagiri, R.; Scott, C. E. Polym Eng Sci 2001, 41, 1310.
32. Lin, B.; Sundararaj, U. SPE ANTEC Tech Papers 2001, 59, 3056.
33. Scott, C. E.; Joung, S. K. Polym Eng Sci 1996, 36, 1666.
34. Ratnagiri, R.; Scott, C. E. Polym Eng Sci 1998, 38, 1751.
35. Ratnagiri, R.; Scott, C. E. Polym Eng Sci 1999, 39, 1823.
36. Taylor, G. I. Proc R Soc London A 1932, 138, 41.
37. Wu, S. Polym Eng Sci 1987, 27, 335.
38. van Krevelen, D. W. Properties of Polymers, 2nd ed.; Elsevier Scientific: Amsterdam, 1976.
39. Sundararaj, U.; Dori, Y.; Macosko, C. W. Polymer 1995, 36, 1957.
40. Favis, B. D.; Chalifoux, J. P. Polym Eng Sci 1987, 27, 1591.
41. Wu, S. In Polymer Handbook, 3rd ed.; Brandrup, J., Immergut, E. H., Eds.; Wiley: New York, 1989.
42. Sundararaj, U.; Macosko, C. W. Macromolecules 1995, 28, 2647.
43. Sundararaj, U.; Macosko, C. W.; Nakayama, A.; Inoue, T. Polym Eng Sci 1995, 35, 100.
44. Bafna, S. S.; Sun, T.; Baird, D. G. Polymer 1993, 34, 708.
45. Kim, W. N.; Burns, C. M. Macromolecules 1987, 20, 1876.
46. Meier, G.; Vlassopoulos, D.; Fytas, G. Europhys Lett 1995, 30, 324.